Developing gold nanotubes as photoacoustic contrast agents

IOP Conf. Series: Journal of Physics: Conf. Series 1151 (2019) 012018 doi:10.1088/1742-6596/1151/1/012018

Developing gold nanotubes as photoacoustic contrast agents

Sunjie Ye[1, 2*], Gemma Marston[2], Alexander F Markham[2], Patricia Louise Coletta[2] and Stephen D Evans[1]

[1] School of Physics and Astronomy, University of Leeds, UK
[2] Leeds Institute for Biomedical and Clinical Sciences, University of Leeds, UK

[*]Email: s.ye@leeds.ac.uk

Abstract. Photoacoustic imaging (PAI) combines the spectral selectivity of laser excitation with the high resolution of ultrasound imaging, representing a noninvasive modality that holds remarkable potential for clinical translation. In particular, multispectral optoacoustic tomography has emerged has an innovative PAI technology, which enables high detection specificity by resolving multiple spectral signatures through tissues and accurately decomposing the biodistribution of relevant molecules from non-specific background contributions. Key criteria for developing PAI contrast agents include strong absorbance in the near-infrared (NIR) tissue transparent region and low toxicity. In this study, we have fabricated gold nanotubes (Au NTs) with controlled length and NIR absorption for the application as in vivo MSOT contrast agents. The length control relies on the synthesis of silver nanorod template under certain growth conditions. The Au NTs were coated with a layer of biocompatible polymer, poly(sodium 4-styrenesulfonate) (PSS), to ensure colloidal stability and low cytotoxicity. The PSS-Au NTs have shown excellent MSOT signal enhancement on tissue-mimicking phantom and in vivo, demonstrating the potential for further development towards a theranostic nanoplatform integrating PAI capability and therapeutic functions.

1. Introduction

Photoacoustic imaging (PAI) has been explored as an informative and promising imaging technology for medical diagnosis. It is based on photoacoustic effect, follows a “light in and sound out” manner. More specifically, the laser absorption by the target region gives rises to rapid thermal expansion, leading to the production of acoustic waves, which are detected by ultrasonic transducers to be processed into images. PAI is a non-ionizing and non-invasive modality integrating the high contrast of optical imaging with the high resolution and deep tissue penetration of ultrasound imaging, beneficial for clinical translations [1]. Recent advances of fast-tuning lasers have boosted the emergence of multispectral optoacoustic tomography (MSOT), a PAI technique which illuminates target at multiple wavelengths and enables the identification of the contributions from various photo-absorbers by spectral unmixing. Compared with imaging methods using single- or two- wavelength illumination, MOST offers a more sensitive and robust approach to quantitative volumetric imaging. The uses of PA contrast agents (PACAs) can facilitate the acquisition of remarkably richer information at the region of interest by MSOT imaging [2]. Gold nanomaterials have great potential to be exploited as PACAs, owing to their inherent and geometrically induced optical properties. The control of localized surface plasmon modes of gold nanomaterials allows the fine-tuning of their optical properties [3]. The signal-to-noise ratio of PAI can be substantially amplified by carefully selecting the excitation laser wavelength in the NIR region to minimize light attenuation [4]. Therefore, intense research has focused on fabricating NIR-absorbing gold nanomaterials. As a promising PACA for biomedical and clinical applications, gold

nanotubes (Au NTs) offer appealing advantages, including the hollow core which can lower the heat capacity to allow better pulse heating [5], coupled with the elongated shape which improves targeting efficiency [6]. However, the majority of previously reported Au NTs have micro-sized lengths and lack optical absorption in NIR region, thereby limiting their PA capability and other biomedical applications.

In this study, we fabricated Au NTs with controlled length (ca. 370 nm) and NIR absorption, though the galvanic replacement reaction between $HAuCl_4$ and silver nanorods (Ag NRs). The Au NTs were subject to the surface modification of PSS coating, which provides colloidal stability and low cytotoxicity. MSOT was used to assess the PA capability of the PSS-Au NTs on tissue-mimicking phantom and in living mice.

2. Methodology

2.1. Materials

Gold (III) chloride trihydrate (520918), cetyltrimethylammonium bromide (CTAB, H6269), ammonium hydroxide solution (NH_3 in H_2O) were purchased from Sigma-Aldrich. Silver nitrate (11414), Trisodium citrate, anhydrous (45556), L-(+)-Ascorbic acid (A15613) were purchased from Alfa Aesar. Poly(sodium4-styrene sulfonate), MW 70, 000 (PSS, 10328550), sodium borohydride ($NaBH_4$, 10599010), hydrochloric acid (37%, UN1789) and nitric acid (70%, UN2031) were purchased from Fisher Scientific. All chemicals were used without further purification.

2.2. Characterizations

The UV-vis spectrum was recorded on a Perkin-Elmer Model Lambda35 spectrophotometer. Scanning Electron Microscopy (SEM) imaging was performed on a LEO 1530 Gemini FEGSEM, with the sample prepared by placing 5 μL dispersion of nanoparticle (in Milli-Q) onto an aluminium substrate and drying under room temperature naturally. Transmission Electron Microscopy (TEM) imaging was conducted using TEM; Tecnai™ G^2 Spirit TWIN / BioTWIN with an acceleration voltage of 120 kV. The sample was prepared by dropping 5 μL dispersion of nanoparticle (in Milli-Q) onto a carbon-coated copper grid and dried at room temperature naturally. The concentration of AuNTs in the aqueous dispersion was measured with an atomic absorption spectrometer (AAS, Varian 240fs).

2.3. Reaction Preparation

Vials and stir bars were treated with aqua regia (nitric acid and hydrochloric acid in a volume ratio of 1:3), rinsed with Milli-Q water, and dried in an 80 ºC oven before use. Once dried, the flasks cooled to room temperature prior to the addition of any reactants.

2.4. Synthesis of Ag NRs

2.4.1. Preparation of Ag seeds

The aqueous solution of $AgNO_3$ (120 μL, 10 mM, freshly-prepared) and aqueous solution of trisodium citrate (250 μL, 5 mM) were sequentially added into 4.625 mL Milli-Q to generate 5 mL solution with a final concentration of 0.25 mM $AgNO_3$ and 0.25 mM trisodium citrate, into which an aqueous solution of $NaBH_4$ (0.3 mL, 10 mM, freshly-prepared and kept at 4ºC for 3h before use) was injected with magnetic stirring. Stirring was stopped after 30 s. The as-obtained seed dispersion was incubated at 21ºC in dark for two hours.

2.4.2. Growth of Ag NRs

The aqueous solution of $AgNO_3$ (100 μL, 8 mM, freshly-prepared) and aqueous solution of ascorbic acid (200 μL, 100 mM), Ag seeds (50 μL) were sequentially added into PSS aqueous solution (3.72 mL, 21.7 mM, the concentration of PSS was calculated according to its monomer unit) without stirring. Following a 10-minute undisturbed growth at 30ºC, the reaction products were collected by centrifugation at 3005g for 10min followed by removal of the supernatant. The Ag NR pellet was re-dispersed in Milli-Q.

2.5. Fabrication of Au NTs

The as-prepared Ag NRs were washed with Milli-Q for 3 times *via* centrifugation (3005 g for 8 mins for each time). The final Ag NR pellet was mixed with 165 μL of CTAB aqueous solution (20 mM), and then subjected to sonication treatment for 15mins. The aqueous solution of $HAuCl_4$ (0.02 M, 10 μL) was dropwise added to the CTAB-Ag NR solution. The reaction was allowed to proceed at room temperature for 30 min with magnetic stirring. The obtained solution was centrifuged at 4696 g for 8 mins. Following the removal of supernatant, the pellet was washed with CTAB aqueous solution (10 mM) and $NH_3{\cdot}H_2O$ (33%) subsequently, then redispersed in 200 μL $NH_3{\cdot}H_2O$ and kept for overnight to further remove the AgCl (some Ag was also removed by treatment with $NH_3{\cdot}H_2O$). The mixture was centrifuged and washed with CTAB aqueous solution (10 mM) twice. The final product of Au NTs was collected in Milli-Q. The synthesis was scaled up by 20-fold to yield the Au NTs for *in vivo* studies.

2.6. Surface Modification with Poly(sodium 4-styrenesulfonate) (PSS)

The dispersion of CTAB-Au NTs (O.D. ~1) was added dropwise into the aqueous solutions of PSS (10 mg/mL) and NaCl (5 mM) in a 1:1 volume ratio and allowed to react for 24 h with magnetic stirring. The products were then collected by centrifugation (4696 g, 15 mins), the supernatant was decanted, and the Au NTs were redispersed in an aqueous solution of unadulterated PSS (1mg/mL, the same volume as the original suspension of CTAB-Au NTs). The centrifugation (4696 g, 15 mins)-redispersion cycle was repeated twice to produce PSS-coated Au NTs suspensions with minimal cytotoxicity. The resultant PSS-Au NTs dispersion was centrifuged (4696 g, 15 mins) and redispersed in Milli-Q for future use.

2.7. MSOT imaging

A real-time MSOT system was used in this study (MSOT in Vision 128, iThera medical Germany).

2.7.1. On tissue mimicking phantom

The phantom was provided by iThera, judiciously designed to mimic the optical properties of tissues. It has a cylinder shape with a diameter of 2 cm, and 2 inner cylindrical channels. Each channel has a diameter of 3 mm and ~ 200 μL capacities, with one holding the control medium and the other for the contrast agent, as shown Scheme 1. The phantom tests were performed for PSS-Au NTs dispersion with concentration of 2, 4, 6, 8 and 10 μg/mL.

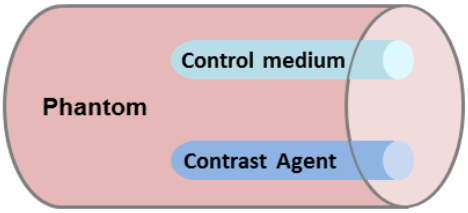

Scheme 1. Schematic representation of tissue-mimicking phantom.

2.7.2 In vivo Photoacoustic Imaging

All experiments were performed following local ethical approval and in accordance with the Home Office Animal Scientific Procedures Act 1986. The animal was anesthetized with isofluorane and placed in supine position inside the imaging chamber. 200 μL of PSS-Au NTs (25 μg/mL) was injected *via* a catheter into the tail vein of anaesthetized mouse and the probe signal was record at different time points post the injections. The laser excitation wavelengths of 715, 730, 760, 800, 830, 850 and 900 nm were selected corresponding to the major turning points in the absorption spectra of PSS-Au NTs, oxy- and hemoglobin.

3. Results and discussion

The length of Ag NRs is determined by the reaction parameter including seed amount and growth temperature [7]. Figure 1 shows a typical SEM image of Ag NRs prepared with 50 μL Ag seeds at 30 ºC. The Ag NRs possess a uniform diameter of ca. 50 nm. The length distribution was analysed by counting 300 nanorods, demonstrating the average length is 372 nm with a variation of 119 nm.

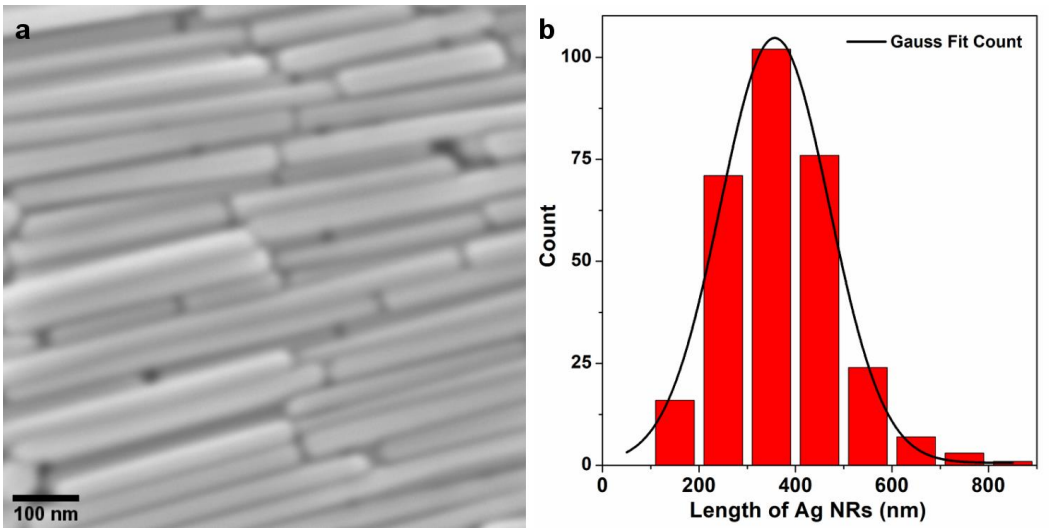

Figure 1. (a) a representative SEM image of Ag NRs. (b) Length distribution of Ag NRs (by counting 300 nanorods)

Au NTs were prepared via the galvanic replacement reaction of the sacrificial Ag NRs and $AuCl_4^-$ ions [8]. Following the addition of $HAuCl_4$ into the dispersion of Ag NR dispersion, the galvanic reaction (See Reaction 1) and Kirkendall effect cooperatively resulted in the generations of Au NTs with hollow interiors and porous walls.

$$3Ag\,(s) + AuCl_4^-(aq) \rightarrow Au(s) + 3Ag^+(aq) + 4Cl^-(aq) \quad (1)$$

Figure 2(a) shows a typical TEM image of synthesized Au NTs (Average length: 372 nm). The center part of each nanostructure is less dense, i.e. having lower contrast, than the edges, suggesting the presence of hollow cavity. The Au NTs displays even walls with pinholes. The wall thickness is approximately 6 nm, about one tenth of the Ag NR diameter, which agrees well with the stoichiometric relation (*according to Reaction 1,* 3 Ag atoms are replaced by 1 Au atom). Importantly, the Au NTs display SPR-associated absorbance peaks around 800 nm, ideally in the NIR region, demonstrating the desired optical properties for uses as PACAs.

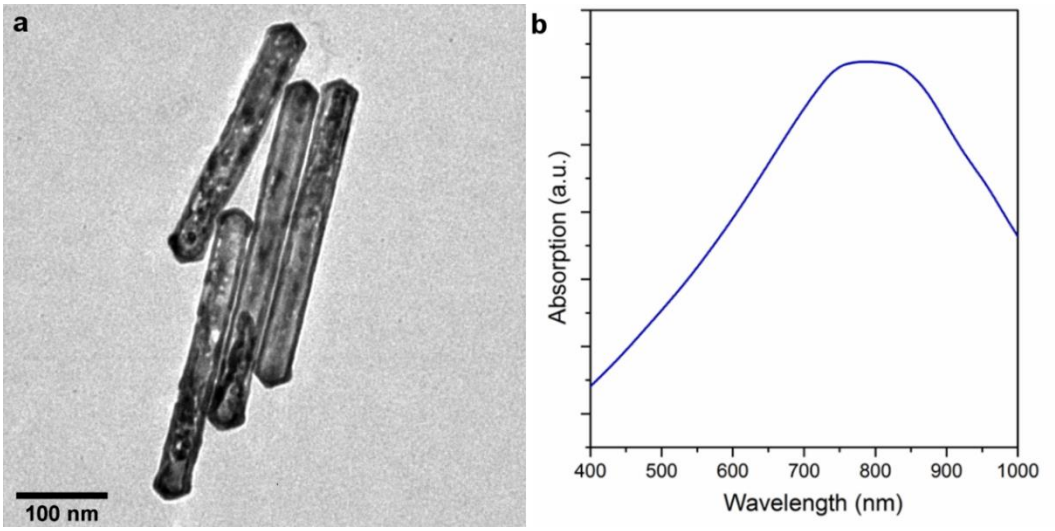

Figure 2. (a) A representative TEM image and (b) UV-vis spectrum of Au NTs

The synthesis protocol of AuNTs involved CTAB, which is notoriously known to have high toxicity. On the other hand, the removal of CTAB tends to cause undesired aggregation of nanoparticles. In addition, the CTAB-Au NTs suffer from poor colloidal stability in buffer medium, undergo agglomeration and precipitation with time, which also restrict their biomedical functions. As such, we performed surface modification by coating the positively charged CTAB-Au NTs with negatively charged sodium polystyrenesulfonate (PSS), which is widely used as a nontoxic agent in commercially-available products and generally regarded as a safe additive [9]. After the treatment with PSS, our PSS-Au NTs demonstrated good colloidal stability in serum-containing medium and low cytotoxicity, making them more suitable for being exploited as PACAs [7].

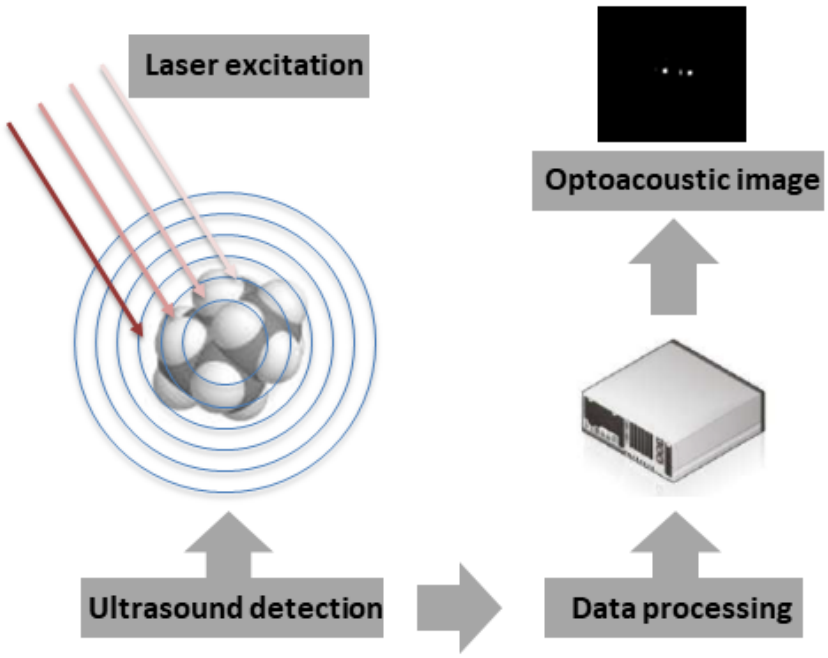

Scheme 2. Schematic illustration of the principle of MSOT.

Motivated by the above-mentioned favorable features of the PSS-Au NTs, such as appropriate length, NIR absorption and good biocompatibility, we further evaluated their PA capabilities using MSOT,

which is well suited for detecting probes in the NIR window. Scheme 2 depicts the principle of MSOT: Pulsed laser illuminates the region of interest (ROI) at multiple-wavelengths and creates transient photon fields in the ROI, producing optoacoustic responses which are collected by acoustic detectors in the form of digital signals. By modeling photon and acoustic propagation in tissues and using inversion methods, images can be reconstructed and spectrally unmixed to identify the contributions of photo-absorbers in the ROI, to generate separate images corresponding to each photo-absorber.

We first performed tissue-mimicking phantom tests to measure MSOT signals of PSS-Au NTs with different concentrations in aqueous solution. The intensity of MSOT signal at 800 nm excitation, the plasmon absorbance peak of PSS-Au NTs, is selected for plotting. The PA signal enhances with the increase of PSS-Au NT concentration and shows a linear correlation (R^2= 0.9978). Notably, the MSOT signal of PSS-A NTs can be well resolved at the concentration as low as 2 μg/mL, demonstrating the excellent photoacoustic capability of our PSS-Au NTs through the highly efficient excitation of NIR-SPR mode.

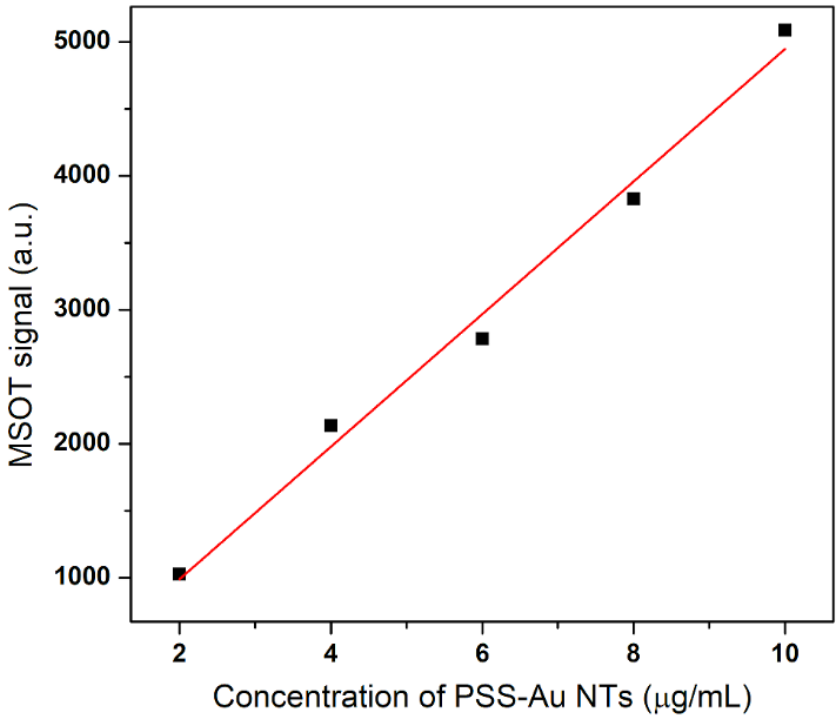

Figure 3. Correlation of MSOT signal intensity of PSS-Au NT aqueous dispersion with concentrations.

We further investigated the effectiveness of PSS-Au NTs as *in vivo* PACAs using MSOT. A 200 μL bolus of PSS-Au NTs (25 μg Au/mL) was injected intravenously into healthy nude mice and images were collected at different time points post-injection. The reconstruction and processing of the raw data using spectral unmixing algorithms allow direct and reliable detection of PSS-Au NTs in living mice. Figure 7 shows processed *in vivo* transverse single-slice MSOT images. Strong *in vivo* MSOT signal associated with PSS-Au NTs was detected in the liver and gradually intensifies with time, from 0 to 18 min post the injection. These results reveal that the PSS-Au NTs can be used as effective PACAS for in vivo imaging, and MSOT imaging can be used for real-time monitoring the locations of these PSS-Au Nanotubes.

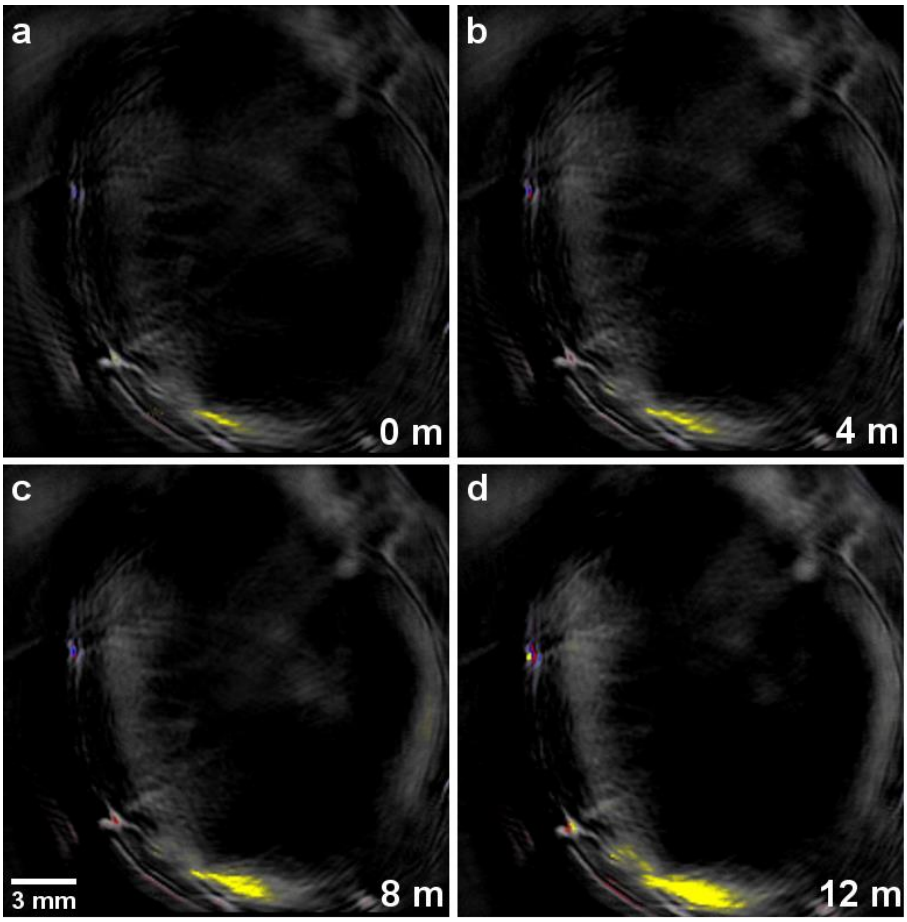

Figure 4. *In vivo* MSOT images (single wavelength 800 nm) of transverse single slice corresponding to spleen–liver region at different time points post injection: (a) 0 min (m), (b) 4 m, (c) 8 m and (d) 12 m. The signal in the yellow channel represents the signal from PSS-Au NTs.

4. Conclusion

This study presents the length-controlled fabrication and surface modification of Au NTs. The PSS-Au NTs have demonstrated ideal features to explore their potential applications as effective PACAs, which may also combine the therapeutic functions (e.g. photothermal therapy and drug delivery) of Au NTs to form a theranostic nanoplatform for monitoring and treating disease in a light-controlled manner.

Acknowledgments

This work was supported by Wellcome ISSF Junior Investigator Development Fellowship. G.M. was funded by EPSRC. The authors acknowledge Thomas Sardella, and Tim Devling from iThera Medical for help in MSOT imaging and data analysis.

Reference

[1] Zackrisson S, van de Ven S and Gambhir S S 2014 Light in and sound out: emerging translational strategies for photoacoustic imaging *Cancer research* **74** 979-1004
[2] Gujrati V, Mishra A and Ntziachristos V 2017 Molecular imaging probes for multi-spectral optoacoustic tomography *Chemical Communications* **53** 4653-72
[3] Dreaden E C, Alkilany A M, Huang X H, Murphy C J and El-Sayed M A 2012 The golden age: gold nanoparticles for biomedicine *Chemical Society Reviews* **41** 2740-79
[4] Song K H, Kim C H, Cobley C M, Xia Y N and Wang L V 2009 Near-infrared gold nanocages as a new class of tracers for photoacoustic sentinel lymph node mapping on a rat model *Nano*

Letters **9** 183-8

[5] Kim J W, Galanzha E I, Shashkov E V, Moon H M and Zharov V P 2009 Golden carbon nanotubes as multimodal photoacoustic and photothermal high-contrast molecular agents *Nature Nanotechnology* **4** 688-94

[6] Kolhar P, Anselmo A C, Gupta V, Pant K, Prabhakarpandian B, Ruoslahti E and Mitragotri S 2013 Using shape effects to target antibody-coated nanoparticles to lung and brain endothelium *Proceedings of the National Academy of Sciences of the United States of America* **110** 10753-8

[7] Ye S, Marston G, McLaughlan J R, Sigle D O, Ingram N, Freear S, Baumberg J J, Bushby R J, Markham A F, Critchley K, Coletta P L and Evans S D 2015 Engineering gold nanotubes with controlled length and near-infrared absorption for theranostic applications *Advanced Functional Materials* **25** 2117-27

[8] Bi Y P and Lu G X 2008 Controlled synthesis of pentagonal gold nanotubes at room temperature *Nanotechnology* **19** 275306 (6pp)

[9] Leonov A P, Zheng J W, Clogston J D, Stern S T, Patri A K and Wei A 2008 Detoxification of gold nanorods by treatment with polystyrenesulfonate *ACS Nano* **2** 2481-8